Modeling Flow Characteristics in Carotid Artery Bifurcation Afflicted with Atherosclerotic Plaques

BEE 4530
Spring 2013
Group 8

Alexandra Braun
Stellie Justin Ford
Marina Shumakovich
Alden Sonnenfeldt

Table of Contents:

Executive Summary

Atherosclerosis is a condition characterized by the hardening of arteries due to the buildup of fatty substances, dead monocytes, and oxidized LDL particles. In advanced cases, atherosclerotic plaques form within artery walls which results in arterial narrowing. In the worst case scenario, the plaque ruptures causing blood clotting and the complete blockage of blood flow. Heart attacks and strokes can result from this event, depending on the site of the blockage. Atherosclerotic plaque rupture in a carotid artery can be catastrophic because a blockage in a carotid will cut off a primary source of blood to the brain.

The goal of this project was to model the blood flow in the bifurcation point of the carotid artery and use COMSOL particle tracing to deposit and add a plaque. Additionally, this project seeks to analyze the effects using aspirin, a blood thinner, as a commonly recommended treatment for patients suffering from atherosclerosis on blood pressure, blood flow, and shear rate in the bifurcation point of a carotid artery with a plaque. Aspirin reduces blood viscosity and facilitate flow, thereby potentially reducing some of the health risks associated with atherosclerosis.

The following assumptions were made to allow for COMSOL implementation: the cardiac output is constant; the artery is rigid and non-compliant; all fluid properties are estimated; blood is a uniform Newtonian fluid; treatments and preventative measures affect only a single aspect of fluid flow; and blood follows laminar flow pattern.

To interpret the model, it was important to consider the potential sources of error. Most of the error originated from the physical approximation from the assumptions listed above. Out of these assumptions, the rigid non-compliant artery simplification was likely the single largest source of error. Additionally, a small amount of error is introduced by COMSOL's interpolation between discrete points.

Despite the error, the results of this project were consistent with experimental data in literature. Particle tracing and velocity profiles demonstrated that a plaque would most likely form in the internal carotid. By iteratively repeating building the plaque using particle tracing as a guide, three representative geometries (34%, 50%, and 55% stenosis) were created to compare to the healthy artery. It was then determined that the reduction in viscosity due to aspirin decreased the shear rate at the walls causing less stress on the artery. Similar effects of blood pressure reduction and exercise increase were observed in this model.

This project could be advanced in the future if the vessels could be modeled as compliant and the blood could be modeled as a non-Newtonian fluid.

Introduction to Atherosclerosis

Atherosclerosis is the stiffening or loss of compliance associated with chronic inflammatory response, smooth muscle cell proliferation, and the accumulation of fatty substances in the intima (Wentzel et al., 2012). Low density lipoproteins (LDL) are widely believed to contribute to plaque formation because small LDL has been shown to increase the risk of atherogenesis. The accumulation of oxidized LDL in macrophages is also directly involved in the accumulation of fatty material and debris that leads to plaque formation (Rajman et al., 1999). Macrophages are not able to digest the oxidized form of LDL, which leads to over accumulation and death of the macrophages in the artery walls. This triggers the inflammatory response and the recruitment of additional macrophages, exacerbating the problem. This inflammatory response results in plaque growth, narrowing of vessel diameter, and increased potential for ischemic stroke (Pruissen et al., 2007).

One of the factors that affect severity of atherosclerosis illnesses is high blood pressure. The ideal blood pressure is in the range of about 73 +/- 2.1 mmHg and 105 +/- 2.9 mmHg (Studinger et al, 2003). Additionally, it is crucial to have the correct blood velocity, which is estimated to be between 10 cm/sec and 50 cm/sec (Wexler et al, 1968), in order to measure pressure and other blood flow factors.

Design Objectives of Modeling the Carotid Artery

In order to treat patients with atherosclerosis, more needs to be known about the progression of the disease and the effectiveness of potential treatments. Using a computer model to study disease progression and treatments is faster, simpler, safer, and less expensive than experimentation.

The goal of this project was to model blood flow near the bifurcation point of the carotid artery, simulate the formation and growth of a plaque, and observe the resulting changes in blood flow characteristics. In order to simulate aspirin treatment, viscosity was varied to determine its effect on blood flow and shear rate along the edge of the plaque.

Extensive clinical research provides background for modeling the carotid artery and its abnormalities. Previous experiments have shown that plaque buildup is correlated with the pressure increase in the artery (Liu et al., 2012). Endothelial shear rate affects the location of plaque formation (Wentzel et al, 2012), suggesting that those are the main factors that need to be examined. Hence, a computer model in simplifies the system of blood flow through the artery and plaque buildup and allows for quick assessment of dynamics and treatments.

Model Formulation

Model Geometry and Schematic

COMSOL was used in order to model the carotid artery as a complex 3D geometry. The COMSOL model was converted from a CAD model obtained from GrabCAD that was itself created from x-ray images. The dimensions of the model were determined and a mesh was created for the geometry as can be seen in Figures 1 and 2. The mesh convergence analysis in Figures B1 and B2 showed that the solution converges at a fine mesh as there is no velocity difference between the fine mesh and the finer mesh. However, due to computational limitations a normal mesh was used in further modeling.

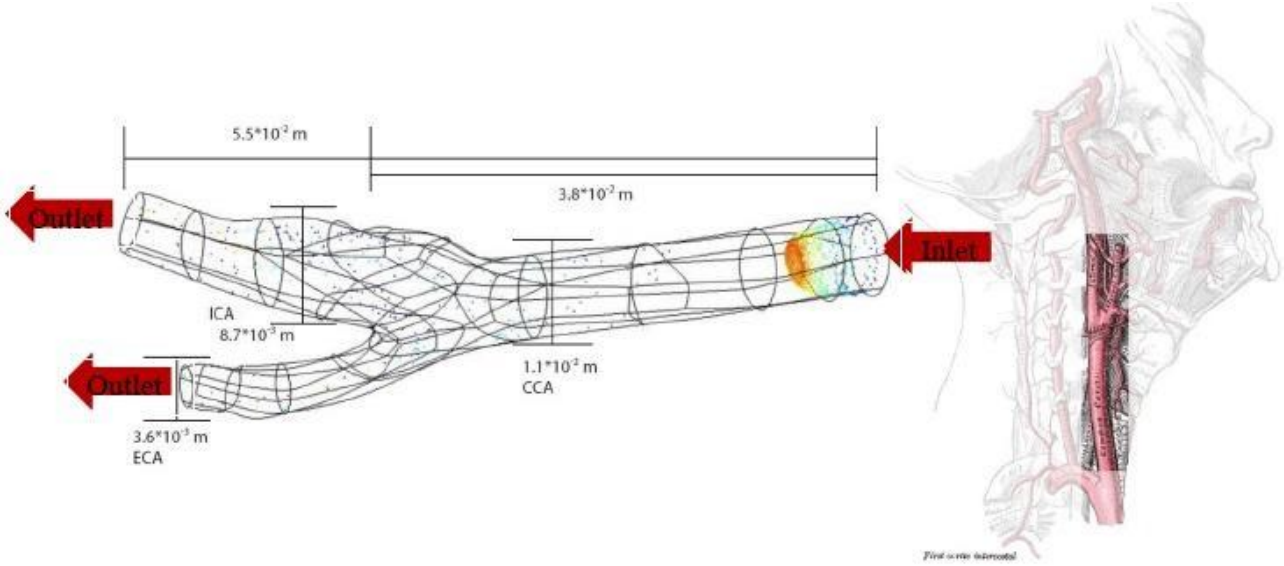

Figure 1: *On the left is a general model of the carotid artery and its dimensions in meters. The colored region on the right end of this model represents the casson flow profile observed near the inlet. The length across the entire carotid is 5.5 cm and 3.8 cm along the common carotid (CCA). The width at the widest point of the CCA is 0.11 mm. The widths of the internal and external carotid arteries (ICA, ECA) are 8.7 mm 3.6 mm respectively. On the right is a drawing of the location and orientation of the carotid in the body. (University of Maryland Medical Center, 2008).*

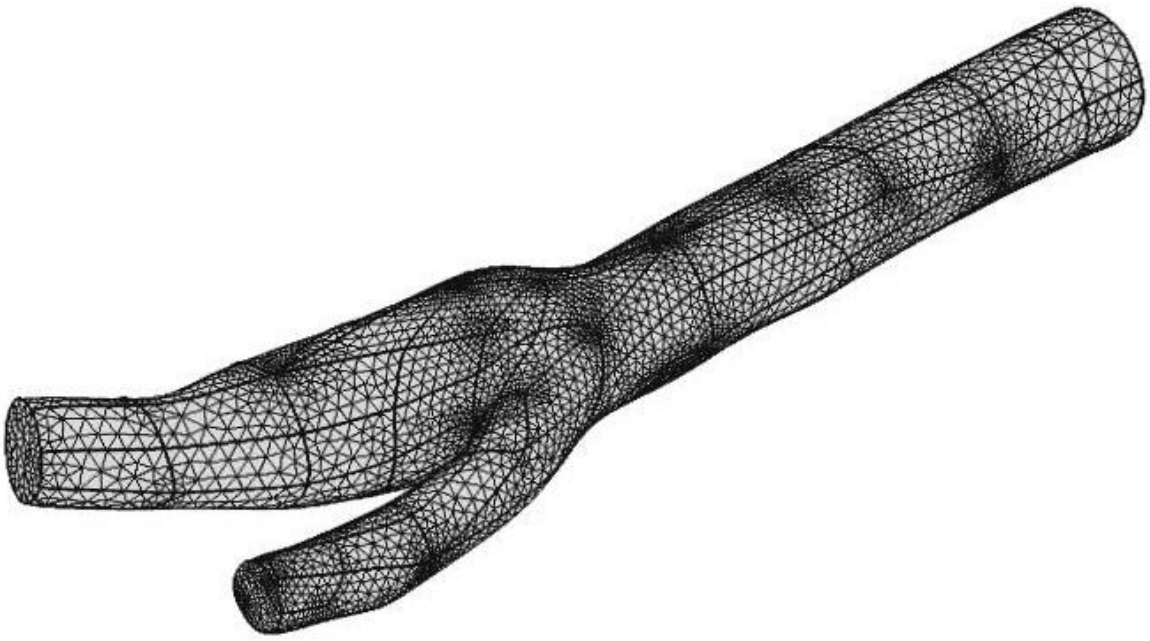

Figure 2: *The 3D mesh of the carotid artery. See table 1 for the details of the mesh shown. The units of the axes are meters. This mesh corresponds to the "normal" mesh in Figure B2 showing the mesh convergence. Although at this point the model has not fully converged yet, this mesh will be used in further calculations because of computing power constraints.*

Model Properties

The assumptions made in the model are listed in Table A1. Zero slip at the walls was assumed in order to facilitate the modeling of velocity and shear profiles. This assumption allowed for a Casson flow model which corresponds to the flow found in actual arteries and is not too computationally intensive. Blood was assumed to follow a laminar flow pattern because it is simpler to model than turbulent flow. Once all parameters were calculated, the Reynolds number showed that the flow was below calculated to be 39.2 as shown in Figure A1, which is much lower than 2300 and hence was truly laminar. Although blood is not a Newtonian fluid, it was assumed to be Newtonian because the artery is a relatively small vessel and hence Newtonian and non-Newtonian models should give similar results. Additionally, Newtonian flow is computationally simpler to model and was therefore used due to limited computing power. The vessel was modeled as rigid and there is no transport through the arterial wall in the model because of the added computational complexity. A function for the probability of the particles sticking to the arterial wall was selected to have probabilities range between zero and one and be inversely proportional to shear rate. Cardiac output was considered constant, based on a healthy person's heart. Finally, it was assumed that treatments affect only one condition at a time because their main effect is more significant and additional factors would add too much computational complexity.

The governing equations can be seen in Table A2. The Navier-Stokes equation was selected as the governing equation for the blood flow because it models the conservation of momentum in the artery with the assumed Newtonian blood flow. The particle tracing model also followed a drag equation which was predefined in COMSOL.

Initial and boundary conditions can be seen in Table A3. The initial and outlet pressures were set to a constant value because they simulated the systemic arterial pressure. The blood inlet velocity was set to a pulsating pattern, as shown in Figure A2, because it is dependent on the heartbeat and the time dependent values for the inlet velocity were taken from Datta et al. (2010). Initial blood velocities were defined to be non-zero only in the z-direction and that were taken from Datta et al. (2010).

The properties of the cardiac cycle and blood properties are shown in Table A4 and were taken from Datta et al. (2010). The time for one cycle was set to 0.75 seconds because that is the time for one heartbeat to occur and hence corresponds to one pulse.

Sensitivity Analysis and Optimization

In an optimization study, pressure was varied with density and viscosity fixed at 1060 kg/m^3 and 0.0035 Pa*s respectively (Figure 3). This pressure analysis indicates that, at standard operating parameters, there was a threshold pressure necessary in order for the characteristic spike associated with a heartbeat to be seen. This fixed outlet pressure, further referred to as systemic pressure, was around 13800 Pa. This optimization also made apparent some of the effects of a defined fluid velocity at the inlet. One of which was a fixed pressure drop across the artery that does not change with the magnitude of systemic pressure. Similarly, the blood pulse is associated with a constant 2000 Pa spike in pressure as long the systemic pressure is above its threshold value.

Sensitivity analysis was performed and different combinations of blood viscosities and densities were tested and the resulting pressures were compared to literature values from (Blackshear et al, 1980) and (Studinger et al., 2003) respectively. Blood density and viscosity were varied jointly from 960 - 1120 kg/m^3 for density with varied intervals, and 0.003-0.00425 Pa*s in intervals of 0.00025 Pa*s for viscosity. This joint sweep was analyzed based on the maximum pressure at 1.55 s, just after the blood pulse at 1.5 s (Figure 4).

Figure 4 gives an information-dense analysis on the viability of certain model parameter combinations. Both higher blood density and higher blood viscosity induced aberrant model behavior. The maximum possible pressure for each set was observable, but combinations with high densities and high viscosities showed a very low maximum pressure of less than 14.5 kPa. This was because with certain combinations, the flow in the channel was not able to develop into a regular pattern such that a

jet of blood was seen in the center of the channel after a pulse. Investigation showed that average pressure during the simulations for aberrant combinations followed a similar pattern to the trials below threshold pressure as seen in Figure 3. In low maximum pressure combinations, the pressure in the carotid never jumped more than 500 Pa above the set systemic pressure.

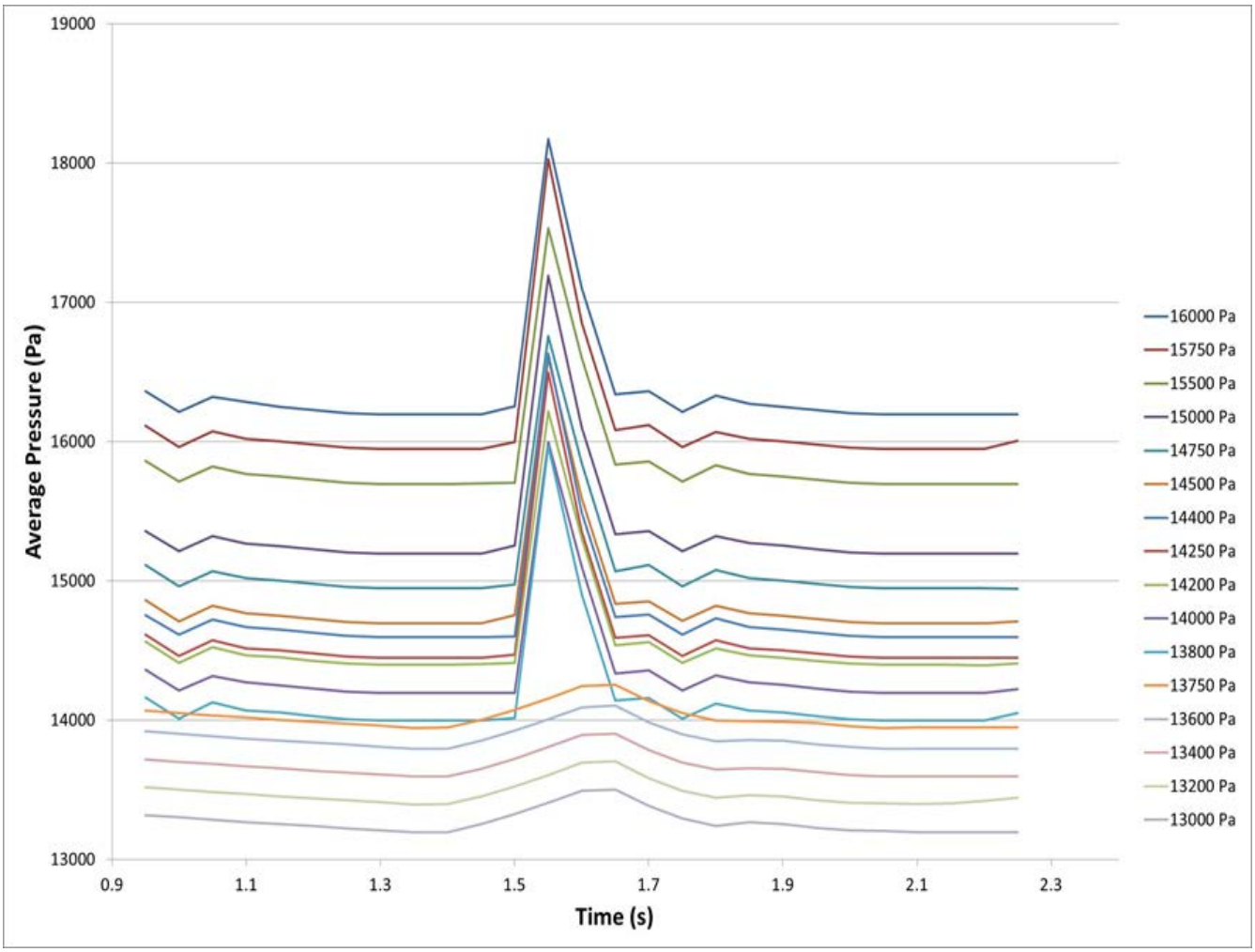

Figure 3*: Systemic pressure (i.e. initial and outlet pressure) was varied to determine the sensitivity of the model to the change in parameters. Plotting average pressure in the carotid shows that systemic pressures 13750 Pa and below cause the model to fail. The lack of a sharp peak in the average pressure indicates that the expected flow pattern never developed. At systemic pressures 13800 Pa and above, the model is functioning properly and the expected flow pattern is developed. Increasing the systemic pressure causes a proportional increase in the average pressure.*

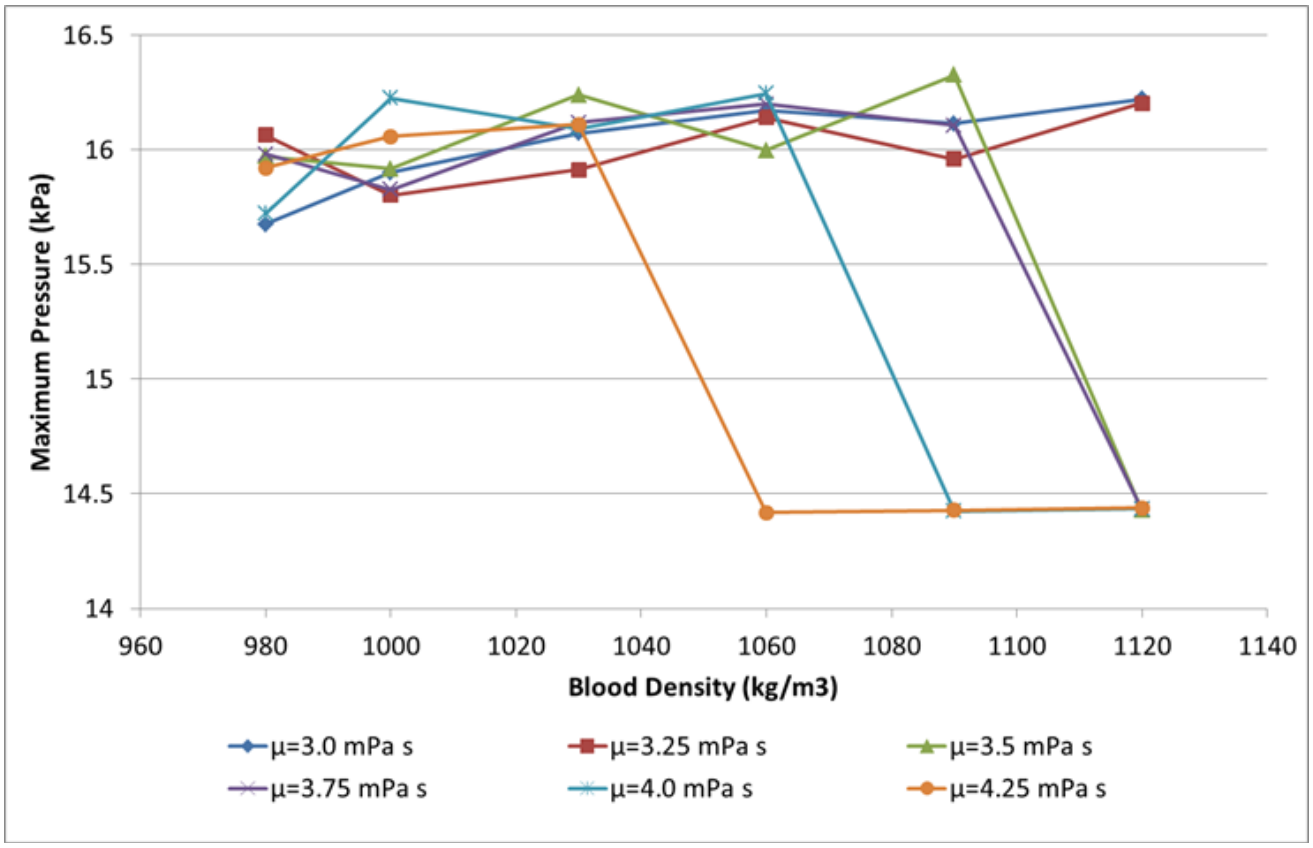

Figure 4: *Maximum pressure across the carotid artery with increasing blood density at different blood viscosities. Through this graph one can see that that at high viscosities and densities, the maximum pressure drops to the minimum physical pressure.*

Plaque Formation

The COMSOL particle tracer was used to represent low density lipoproteins (LDL) present in the blood. LDL are a free floating blood component that, when oxidized, are believed to contribute to the growth of atherosclerotic plaques (Rajman et al., 2001). Based on data on the dimensions and properties of LDL described in Rajman et al., particles with a density of 1038 kg/m^3 and a diameter of 22 nm were chosen for the particle tracing model and particle velocities were derived from the drag equation in Table A2. The probability that an LDL would adhere to the walls of the artery varied inversely with shear rate as seen in Table A1. The model parameters, boundary conditions, and initial conditions were kept consistent with the original flow model.

The region highlighted in Figure 5 was chosen as the initial location of plaque because in that area LDL accumulated there during particle tracing, backflow disrupted the steady flow pattern, sand it was the region of lowest blood velocity. Backflow further influences plaque location via its impact on the behavior of endothelial cells and shear rate. As shown by Wentzel et al. (2012), cells in an area of low shear have much lower expression of atheroprotective genes. There is also an increase of reactive

oxygen in these cells, which is necessary to generate the oxidized LDL that is the cause of plaques. Building the plaque in the internal carotid is also interesting because this vessel supplies blood to the brain and blockage of this vessel could result in a catastrophic stroke.

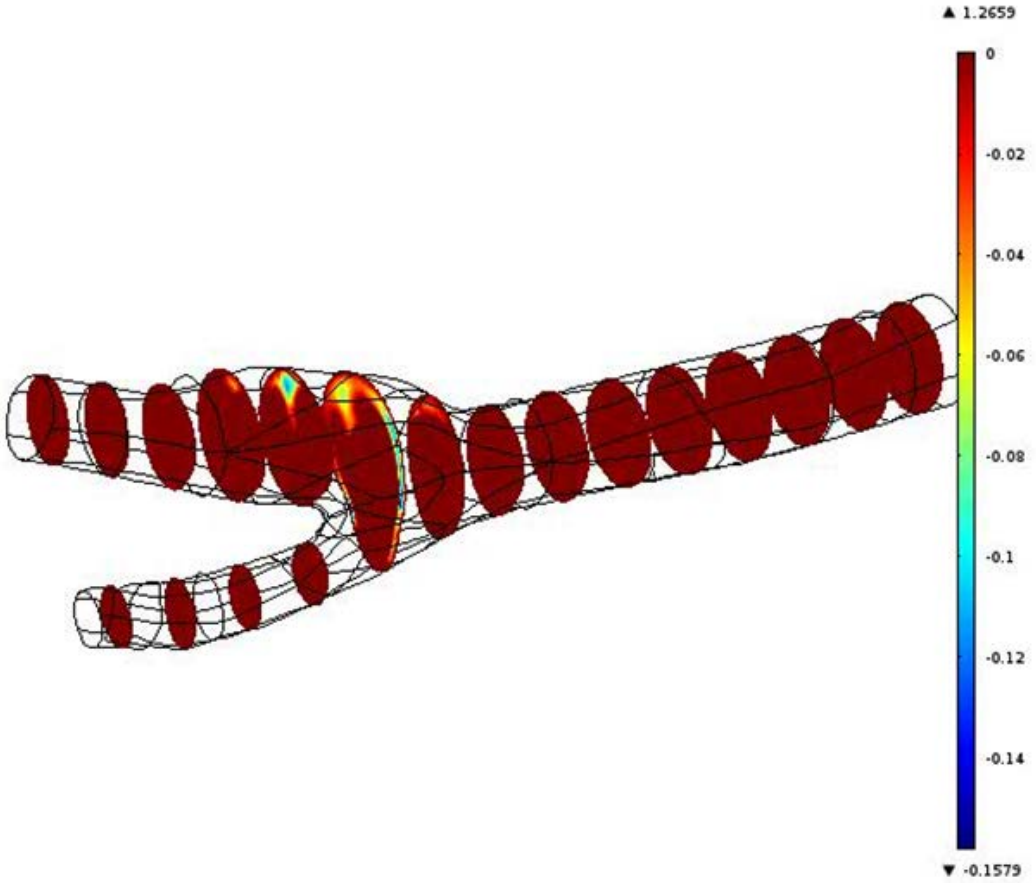

Figure 5: *Backflow that form in the ICA and leads to more plaque formation. The area of backflow is shown in blue. This backflow is consistent with the one seen in Figure 16, which validates the flow pattern generated in this model.*

The plaque was built into the carotid by subtracting pieces of spheres from the geometry. After the initial plaque was placed, the size was increased by using the results of particle tracing (Figure 6) to guide the placement of additional spheres. By iteratively increasing the size of the plaque in this manner the new carotid geometries illustrated in Figure 7 were created. The 34% stenosis plaque was chosen as the start point for experimentation because it was the lowest stenosis where significant changes in flow patterns were observed. The 55% stenosis plaque was chosen as the endpoint because it was the lowest stenosis at which the plaque prevented a steady flow pattern from forming.

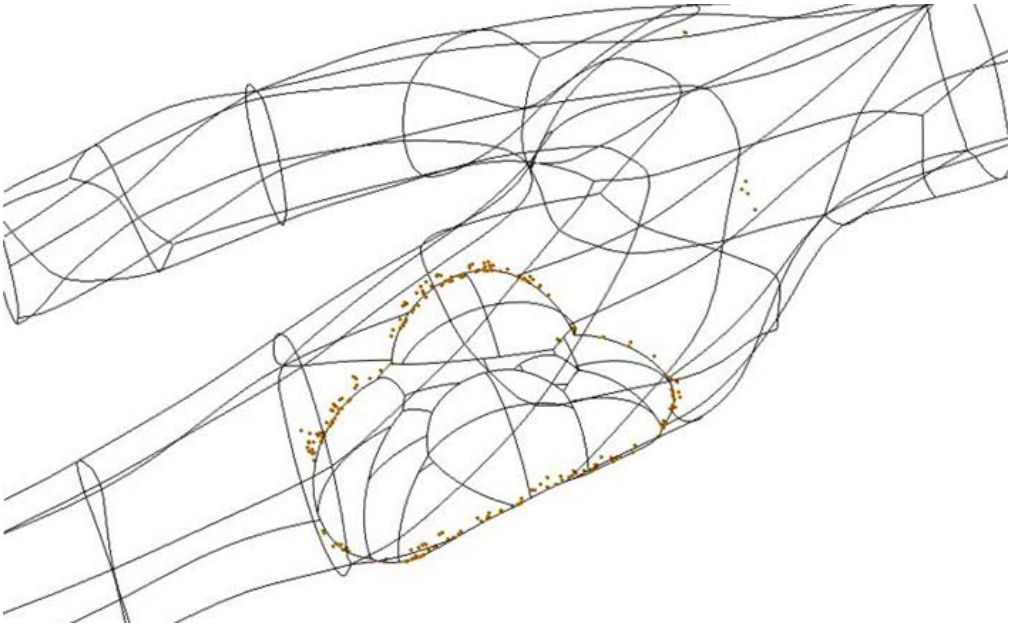

Figure 6: *The end result of particle tracing simulations showing the locations of stuck particles in orange along the edge of the plaque.*

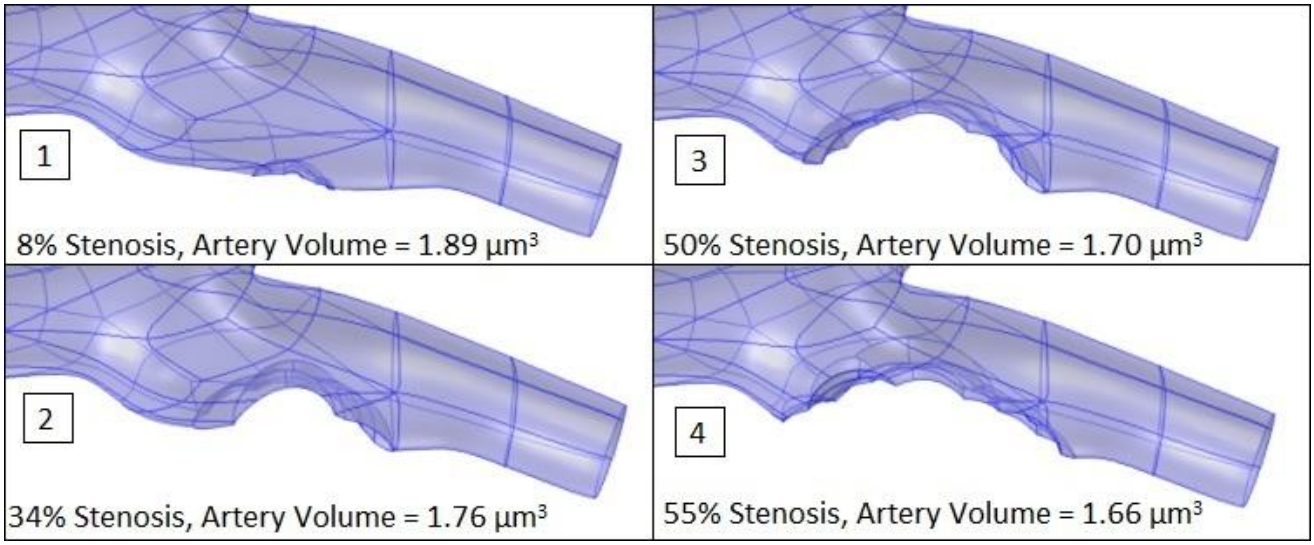

Figure 7: *Four select stages of plaque growth.*

Modeling Aspirin Use

Taking blood thinners such as aspirin is recommended for reduction of blood viscosity in order to reduce systemic pressure and facilitate flow through a partially obstructed artery. Research by Rosenson (2008) showed that taking dipyridamole along with aspirin was more effective than aspirin alone at reducing blood viscosity. For shear rates ranging from 300 to 1000 s^{-1}, blood viscosity decreased by approximately 0.00022 Pa*s as shown in Table A5. Viscosity was decreased from 0.0035

Pa*s to 0.0033 Pa*s in order to model aspirin treatment and shear rate along the edge of the plaque was used to assess its efficacy.

Results and Discussion

Flow characteristics with and without the plaque

Figure 8 is a plot of the average velocity of blood flow through the carotid artery at 2.25s. A flat plateau region of larger velocity was observed at the center of the artery with slower velocities around the edges.

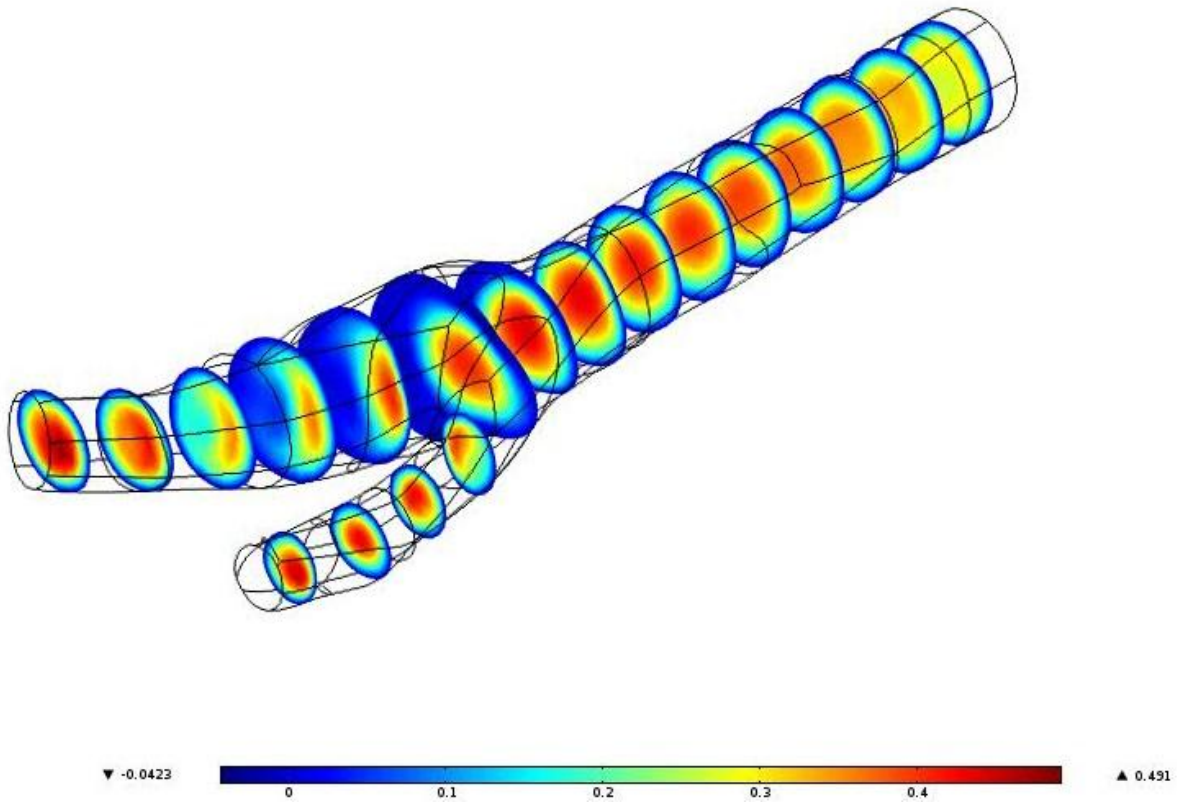

Figure 8: *The velocity profile of blood through the carotid artery. The velocity is highest in the center and lowest at the walls, where it is close to 0m/s. In the larger part of the artery shortly after the bifurcation a large portion of the area has velocities close to 0m/s. The plot was made after 2.25seconds. The units of the axes are meters. This figure can be compared to the model after plaque buildup in order to analyze the effect of atherosclerosis on the blood flow through the carotid artery.*

Figure 9 shows a slice plot of pressure across the carotid artery. At each time point there is a characteristic drop in pressure across the artery related to inlet velocity, however, when compared to literature values absolute pressure was seen to be below the optimal range. Further investigation was done to adjust the model.

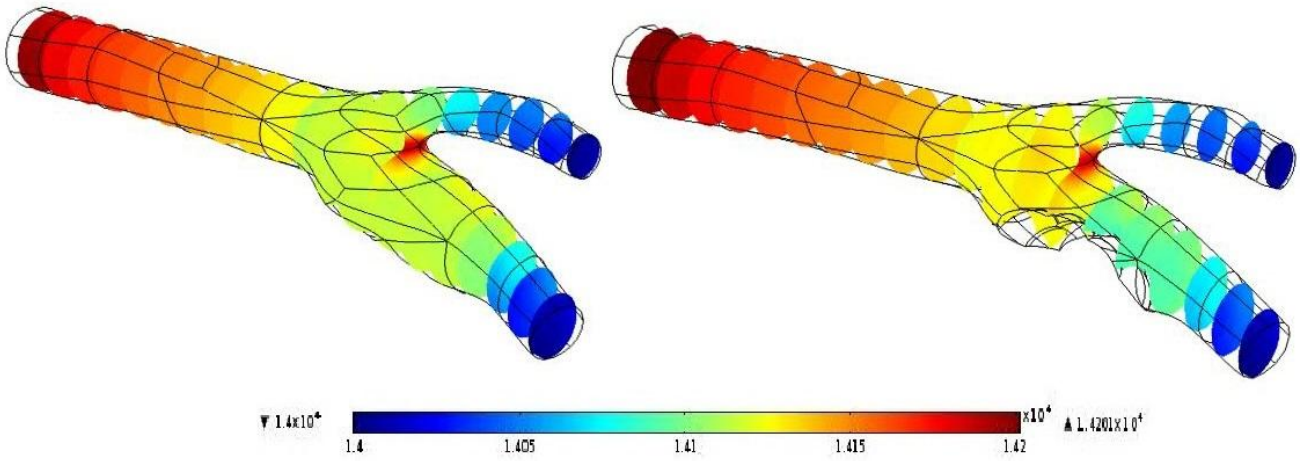

Figure 9: *Both images are slice plots of the pressure across the carotid artery. The pressure is highest at the inlet of the artery as well as at the bifurcation point. At the outlet from the carotid artery, the pressure is the lowest. The plot was made at 2.25seconds. The left is our standard model, and the right is the model at 50% stenosis. Both show the same drop in pressure from inlet to outlet, but the model with the plaque shows a steeper gradient near the bifurcation.*

The plaque affects the flow characteristics in the carotid as expected at 34% and 50% stenosis. Figure 10 illustrates the high degree of similarity between the characteristic flow pattern with and without the plaque. It also shows the direct correlation between maximum velocity and stenosis that one would expect as a constant flow rate is forced through a decreasing cross sectional area. These results suggest that the model is functioning properly with the plaque.

When stenosis rises to 55%, the characteristic sharp peaks of the pulsatile flow pattern cease to develop. Ino-Oka et. al (2009), report that plaques of similar size significantly lower and widen the peak velocity pulse. The 55% stenosis case demonstrates this change but to a much greater degree than expected. This suggests that the model is no longer producing reliable results at this level of stenosis. The rigid boundary assumption, Ino-Oka used a compliant vessel, is likely the source of error that led to this discrepancy. Never the less, the 0-50% working stenosis range is sufficient to achieve the design goals and to simulate the effect of atherosclerosis treatments.

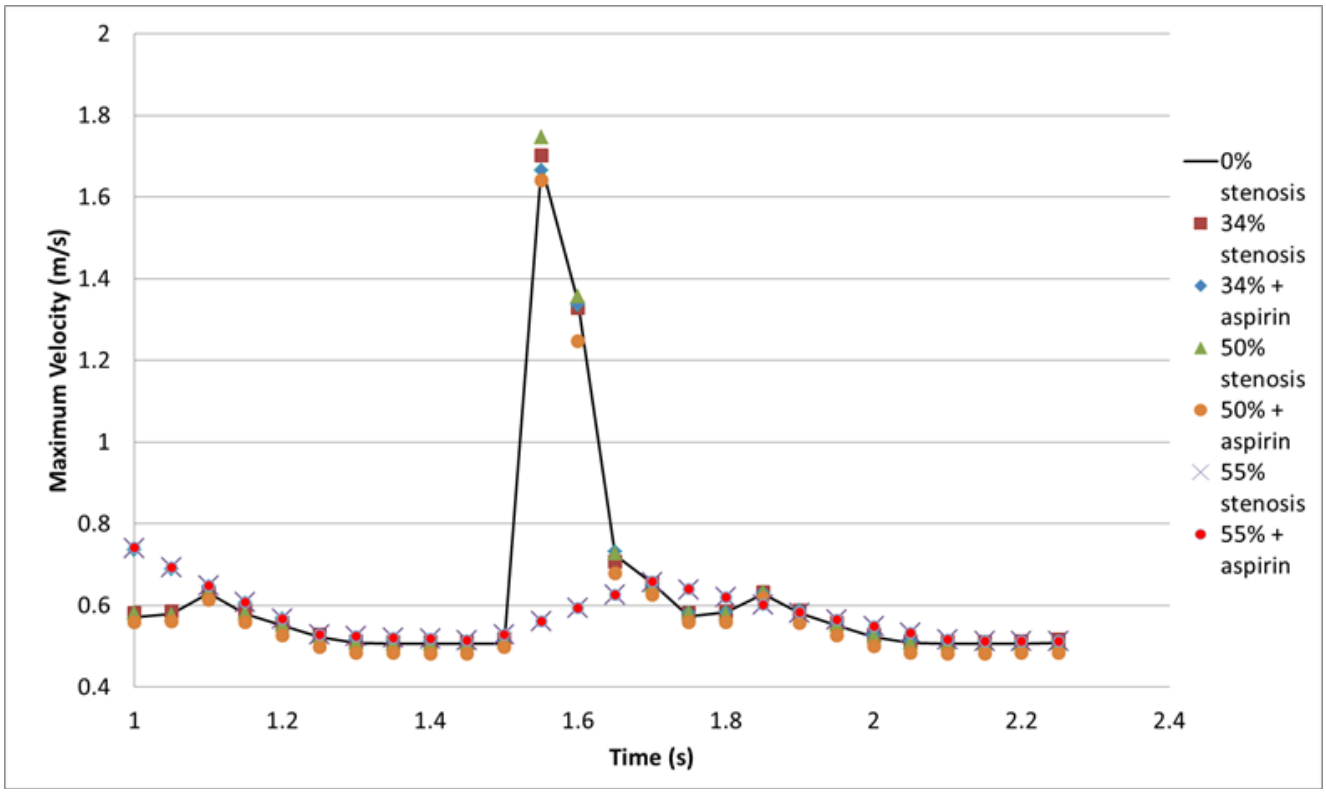

Figure 10: *Comparison plot of maximum velocities in the carotid with plaques of 34, 50, and 55% stenosis in combination with a simulated daily aspirin dose compared to the 0% stenosis baseline.*

Effect of Aspirin on Blood Flow

Aspirin is commonly used as an everyday preventative treatment for patients suffering from atherosclerosis because aspirin, a blood thinner, decreases blood viscosity (Elblbesy et al., 2012). The shear profile along a cross section at the plaque was observed at 50% stenosis with and without the treatment. The resulting shear profile can be seen in Figure 11. The aspirin treatment significantly decreased the shear rate at the walls of the artery especially in the region surrounding the plaque. Shear rate without aspirin reached a maximum of 2140 s^{-1} while the shear rate with aspirin reached a maximum of 1620 s^{-1}. A lower shear rate along the plaque corresponds to a decreased chance of plaque rupture and stroke. This result supports the effectiveness of a daily aspirin dose as a preventative treatment for patients suffering from atherosclerosis.

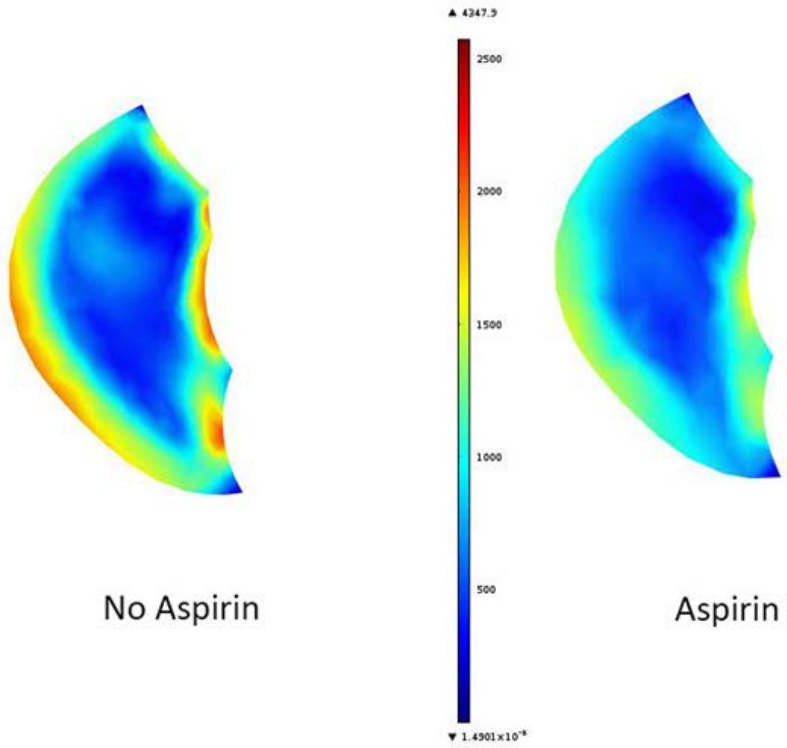

Figure 11: *Shear rate profile at peak velocity over a cross section of the 50% stenosis artery at the plaque. Shear at the walls significantly decreases with aspirin, reducing the chance of plaque rupture.*

Validation of the COMSOL Model

To check the accuracy of the COMSOL model it was decided to look at experimental velocity and pressure data from the literature as well as verifying the presence of backflow near the branch point from another model.

The accuracy of the COMSOL velocity data can be compared to the results reported by Blackshear et al. that were measured using a Doppler flow velocity detector. Velocity range measured was 0.286 - 1.784 m/s. Figure 12 shows the velocities predicted by COMSOL model in the common carotid.

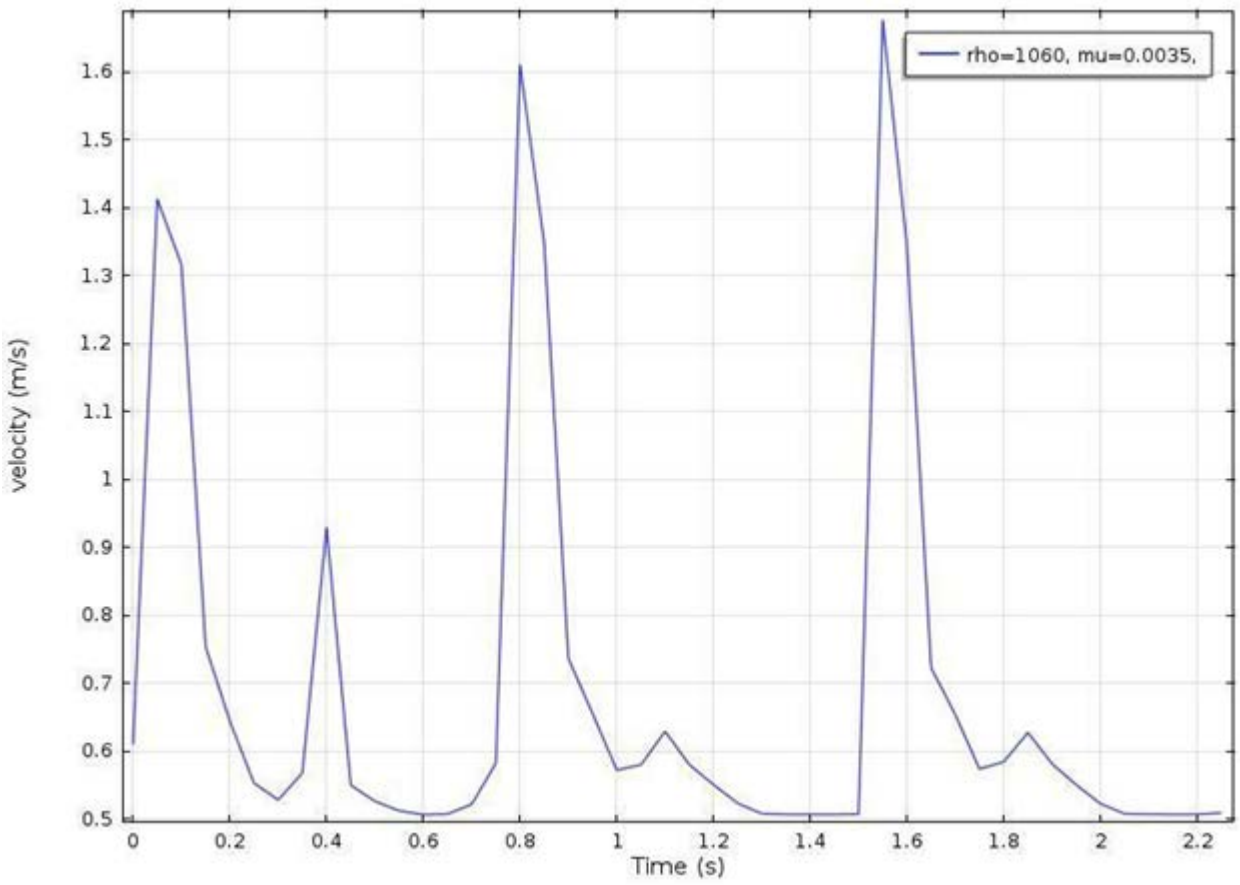

Figure 12*: Maximum velocity across the artery. The pattern is consistent with the pulsating nature of the flow and the velocities stay within the range measured by Blackshear et al. (1980). Additionally, the similar nature of the peaks suggests that the system is close to steady state and the analysis should give consistent results.*

The velocity data obtained by this model are within the ranges measured by Blackshear et al., and the maximum (systolic) pressure (~120 mmHg) is only 5% higher than values seen by Studinger et al. (2003) five minutes after exercising, but is roughly ~14% higher than the average resting systolic pressure of 105 mmHg seen in the same study. Further the pulse pressure seen in this study was half that of Studinger's observed resting value. This is attributed to the lack of compliance in model walls as Studinger describes changes in the carotid diameter of about 1 mm in healthy subjects. This is further validated by the decrease in the range of flow volume in more rigid vessels as shown by Ino-Oka et al. (2009).

In order to complete an accuracy check, literature was examined that looked at similar experimental properties in the carotid artery. Significant backflow was observed near the branch point just after the maximum velocity point in the COMSOL model, as can be seen in Figure 5. This matched the findings of Nguyen et al., shown in Figure 13. The backflow is more consistent at the outer wall of

the internal carotid artery (ICA) near the branch point, but this could be caused by geometrical differences between the compared models.

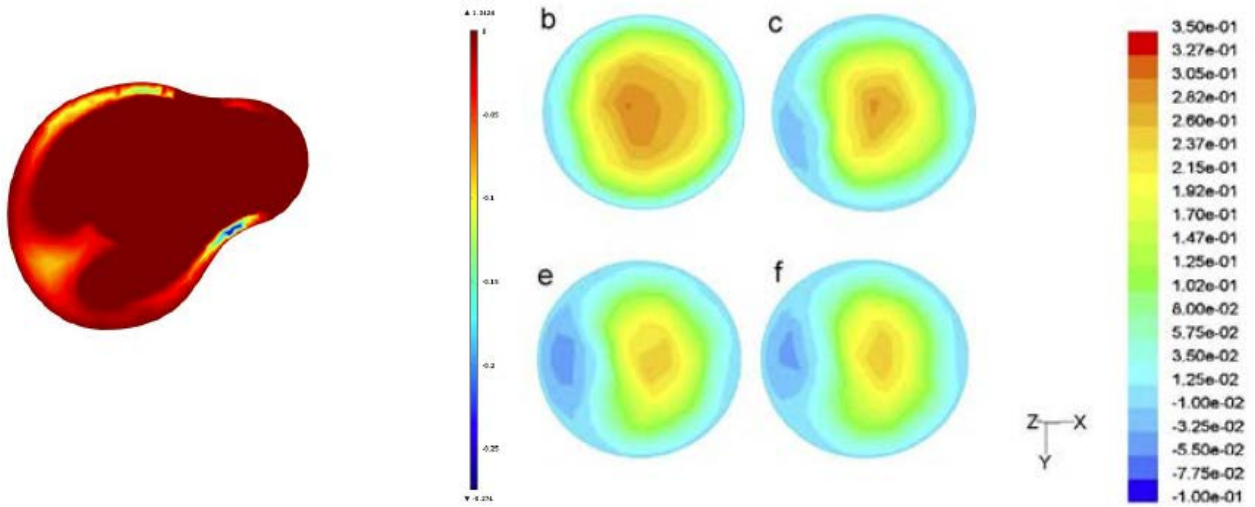

Figure 13: *Literature comparison of the cross section of the backflow pattern obtained in the model (left). The literature velocity contour plots at different locations of the ICA sinus at t = 0.3s with each slice b, c, e, and f moving upstream from the branch point in the internal carotid artery. The color scale is in meters per second (Nguyen et al., 2008).*

Conclusion

Possible model improvements:

While optimization and refinement of the model were completed there are many areas where further improvements can be made. Factors such as computational ability, and complexity of the model caused variations from a fully accurate representation of the carotid artery.

The first improvement that could be made would be to sacrifice computation time and use a model with a higher density mesh. The generated mesh convergence data shown in Figure B1 shows that mesh independent solution is well above the ~100k element mesh chosen for the model and that the difference may cause a significant variation in the model results. Processing and time limitations prevented exploration of higher density meshes, however, the evidence suggests improving the mesh would lead to a more accurate model and could significantly change some of the results.

The rigid boundary assumption was difficult and possibly impossible to avoid given the limitations of the project and COMSOL. However, modeling vessel compliance would significantly improve the model accuracy and is a necessary change if the model was ever implemented in a medical setting. Although atherosclerosis is linked to a loss of compliance in arterial walls, this only occurs after plaque formation. Healthy arteries are elastic and significant change in the volume of the carotid is observed during the cardiac cycle (Ino-Oka et al., 2009 and Studinger et al., 2003). An additional

complication when modeling the growth atherosclerotic plaques is the variation in compliance that would result. An improved model should also address this issue.

Increasing the maximum possible stenosis would be beneficial because the model could be used in a wider variety of applications and because it would better simulate advance cases of atherosclerosis. A compliant model may be the key to surpassing the 50% maximum stenosis value; however, additional changes may also be necessary. Smoothing the geometry of the plaque using continuous lines as opposed to intersecting spheres, for example, would improve the accuracy of the model and could increase the maximum stenosis.

In a more accurate mode, the outlet velocity could also be varied to represent the pulse flow just like the inlet velocity, instead of being constant. That would be a more accurate representation of what is going on in the patient's artery. The inlet velocity could also be set up in a way that it enters the artery with a developed Casson flow profile. This would mimic the fact that blood comes into the artery from the body where it has had time to develop a characteristic flow profile. Finally, blood could be modeled as a non-Newtonian fluid, in which case the governing equation would change but the model would be more representative.

Model Evaluation and Implications

The model successfully achieved the design goals. It produced a realistic representation of blood flow in the carotid artery with and without a plaque that matched other computational models and clinical experiments. Sensitivity analysis showed that there was a wide functional range available in the model parameters to vary during experimentation. Additionally, the working range of 0-50% stenosis provides enough flexibility to simulate most cases of atherosclerosis.

The flexibility of the model makes it possible to use it as a tool to evaluate the effect diet, lifestyle changes, and drug treatments have on blood flow characteristics and the risk of plaque rupture. The impact of a daily aspirin dose was successfully evaluated. The decreased shear and corresponding decreased risk of plaque rupture supports the preventative use of aspirin and illustrates nicely the model's capability of evaluation. The same procedure could be used to evaluate other common treatments and recommendations such as diuretics and decreased salt intake. The model can be easily modified to model anything that affects one or a combination of blood viscosity, density, pressure, or velocity. A refined and improved version of the model could be used as a valuable alternative to expensive animal or clinical studies.

Another potential application of the model is *in vivo* diagnosis of atherosclerosis. Using current technologies, it is difficult and expensive to determine the location of plaques and the extent of stenosis

in living patients. Inexpensive, noninvasive and relatively simple ultrasound procedure, however, are available to determine the velocity of blood flow in arteries (Vennemann et al., 2007). A powerful diagnostic technique could be developed using a comparison of the ultrasound measured velocities with model predicted velocities. The model developed in this project provides an excellent foundation for future arterial blood flow and atherosclerotic models with potentially lifesaving applications.

Acknowledgements
We would like to acknowledge and thank Professor Ashim Datta, Alex Warning, Dr. Traci Nathans-Kelly, and Dr. Rick Evans for all their time, energy and help. Without their guidance this project would not have been possible.

Appendices

Appendix A: Input Parameters and Calculations

Table A1: *List of assumptions made in the model.*

Assumptions
No slip condition: zero blood velocity at artery walls: $u_{wall} = 0\ m/s$
Blood follows laminar flow pattern
Blood is modeled as a Newtonian fluid
Vessel is rigid and non-compliant
No transport through arterial walls
Probability of LDL particles sticking to the wall is only a function of shear rate: $p = 2/(1+e^{(shear\ rate)})$
Cardiac output is constant
Treatments and preventative measures affect only a single aspect of fluid flow

$$\mathbf{Re} = \frac{\rho v L}{\mu} = \frac{(1060\ \mathbf{kg/m^3})(0.005\ \mathbf{m})(0.0259\ \mathbf{m/s})}{0.0035\ \mathbf{Pa*s}} = 39.22 < 2300$$

Figure A1: Calculation for Reynolds's number for carotid artery region prior to bifurcation.

Table A2: *List of governing equations used in the model.*

Governing Equations
Navier-Stokes: $\rho(\frac{\delta u}{\delta t} + u\nabla u) = -\nabla\rho + \mu\nabla^2 u$
Drag Equation: $\frac{d(m_p v)}{dt} = F_t$

Table A3: *List of boundary and initial conditions.*

Boundary and Initial Conditions
Uniform flow rate across inlet= *v*(t) (Datta et al., 2010)
Outlet Pressure= 14,000 Pa (From optimization, see Figure 9)
Values at *t=0s* (from model optimization and refinement)

∘ u_x=0 m/s	u_y=0 m/s	u_z=0.2484 m/s	∘ *P= 14,000 Pa*

Table A4*: Properties of cardiac cycle and material properties of blood*

Input Parameters (Datta et al., 2010)	**Value**
Time for one pulse cycle: t_p	0.75 s
Bloody Density: ρ_{blood}	1060 kgm^{-3}
Blood Viscosity: μ_{blood}	0.0035 Pa*s

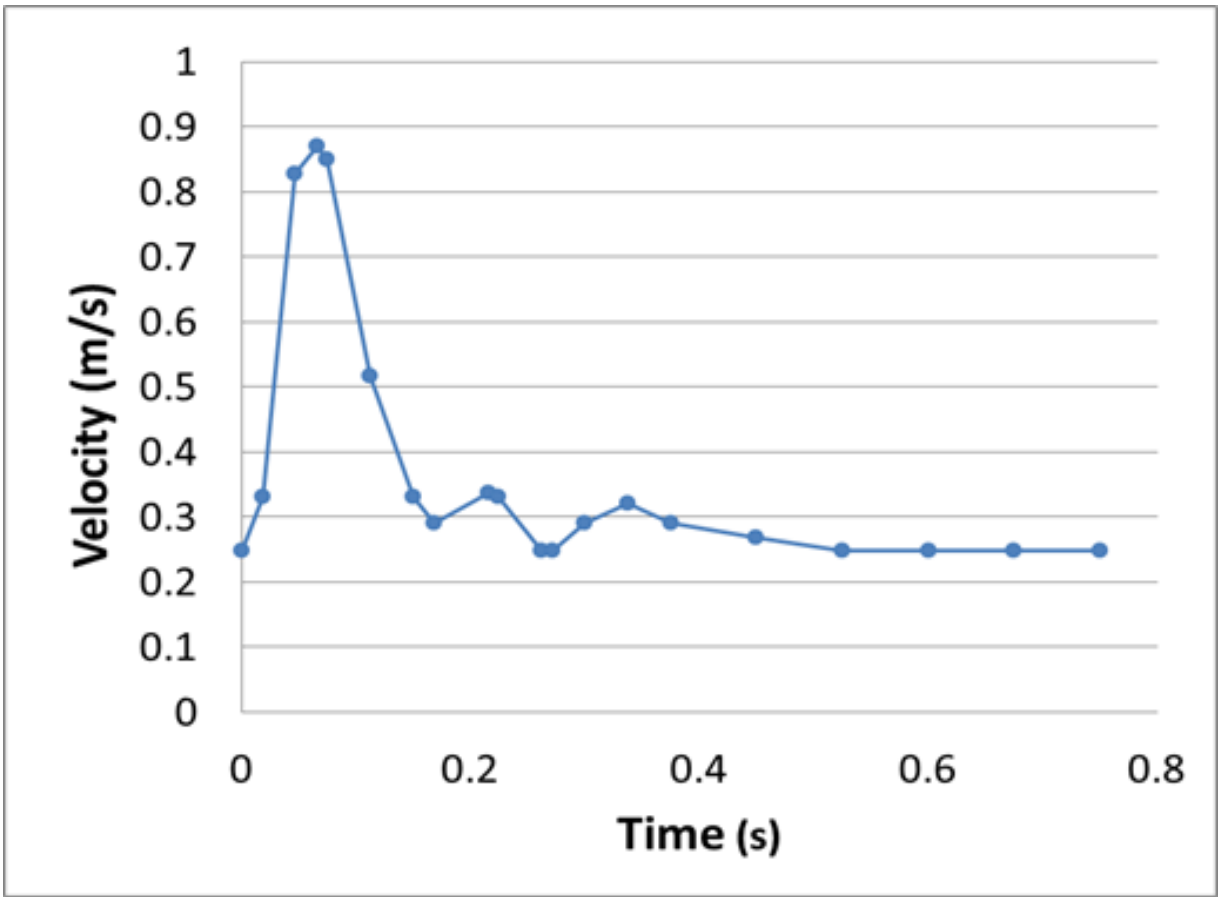

Figure A2*: Plot of inflow velocity as a function of time. Pulsating flow is observed.*

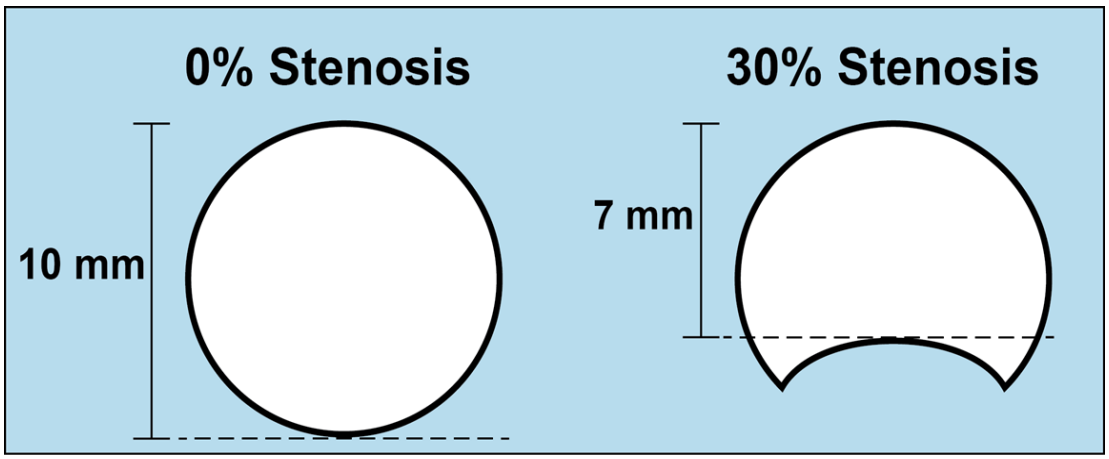

Figure A3*: Percent stenosis is defined as the reduction of diameter of the artery.*

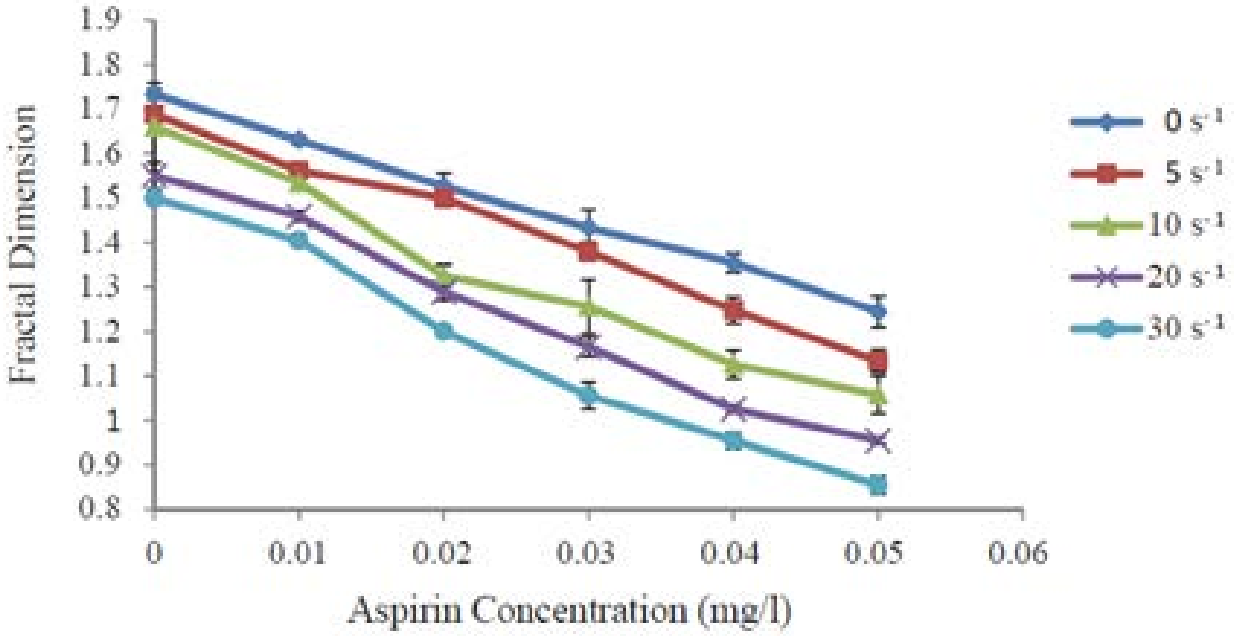

Figure A4: *Relationship between aspirin concentration and fractal dimension, which corresponds to blood viscosity. One can see that more aspirin decreases viscosity. Since this graph also shows relationship with sheer, it will allow us to pick reasonable values for testing conditions (Elblbesy et al., 2012).*

***Table A5**: Effect of aspirin and aspirin/dipyridamole on whole blood viscosity (mPa*s). To simulate the effects of aspirin/dipyridamole treatment, the blood viscosity parameter was varied in the model corresponding to the highlighted value. The Aspirin/dipyridamole combination was chosen as the model aspirin viscosity change because it is known to be the more effective treatment. (Rosenson, 2008).*

	Aspirin (81 mg daily)			Aspirin/dipyridamole (50 mg/400 mg daily)			
Shear rate (s^{-1})	Pre	Post	Change	Pre	Post	Change	*P*-value
1	22.77±7.54	22.70±9.32	−0.07±6.72	22.95±6.39	19.93±6.76	−3.02±4.67	<0.0001
2	15.33±4.49	15.13±5.23	−0.21±3.62	15.48±3.86	13.62±4.10	−1.86±2.79	0.0136
5	9.98±2.42	9.73±2.56	−0.25±1.67	10.09±2.15	9.03±2.27	−1.05±1.51	0.2276
10	7.72±1.60	7.48±1.57	−0.23±1.00	7.81±1.49	7.09±1.54	−0.72±1.00	0.4660
50	5.17±0.77	4.98±0.72	−0.19±0.56	5.23±0.83	4.87±0.77	−0.36±0.49	0.8061
100	4.64±0.62	4.49±0.58	−0.15±0.48	4.68±0.71	4.41±0.66	−0.27±0.37	0.8572
150	4.41±0.55	4.28±0.54	−0.13±0.45	4.44±0.66	4.21±0.61	−0.23±0.33	0.8782
300	4.06±0.50	3.96±0.50	−0.10±0.43	4.11±0.62	3.89±0.56	−0.22±0.29	0.8561
1000	3.64±0.46	3.60±0.46	−0.03±0.44	3.73±0.59	3.51±0.50	−0.22±0.30	0.7731
Hematocrit (%)	41.5± 4.2	41.6±4.7	0.1±1.7	40.8±4.1	39.8± 4.2	−1.0±1.8	0.0446
Fibrinogen (g/L)	3.30±0.7	3.41±0.69	0.11±0.53	3.47±1.06	3.41±0.76	−0.06±0.76	0.4724

Data are presented as the means+standard deviation. *P*-values represent pre-and postdifferences between the two treatments at different shear rates.

Appendix B: Mesh Convergence

***Table B1:** Details of the normal mesh, which is used for further calculations.*

Average element quality	0.7599
Tetrahedral elements	108183
Triangular elements	9902
Edge elements	1635
Vertex elements	132

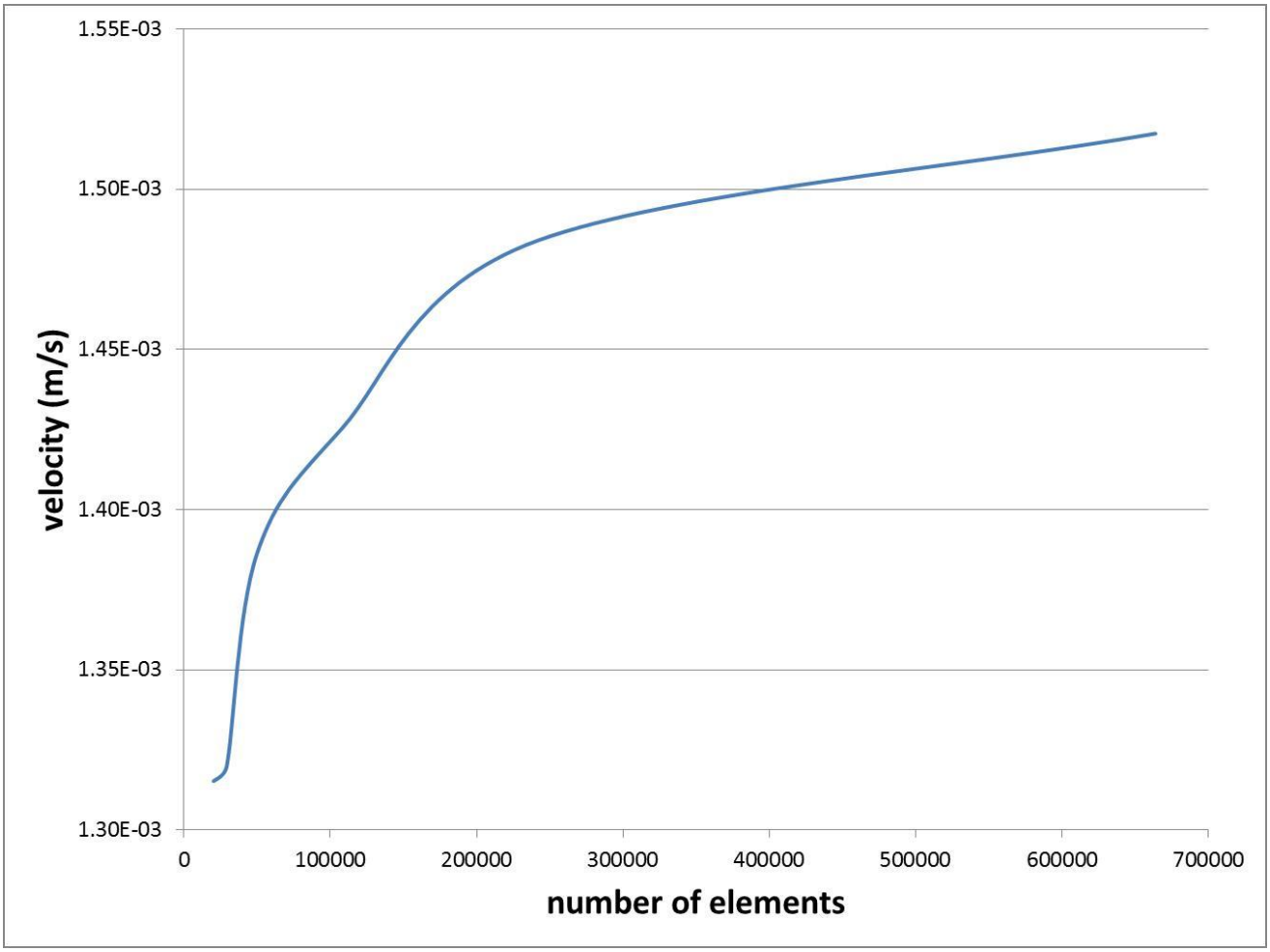

Figure B1: *<u>Mesh convergence comparing velocity and number of elements in the mesh</u>: The above plot shows the mesh convergence for the average velocity versus number of elements at the end of the large outlet vessel after 1.6seconds. The plot shows that convergence occurs at the fine mesh (~241k elements), since the data begin to level off. However, due to the length of computation, normal mesh (~108k elements) was selected for further modeling.*

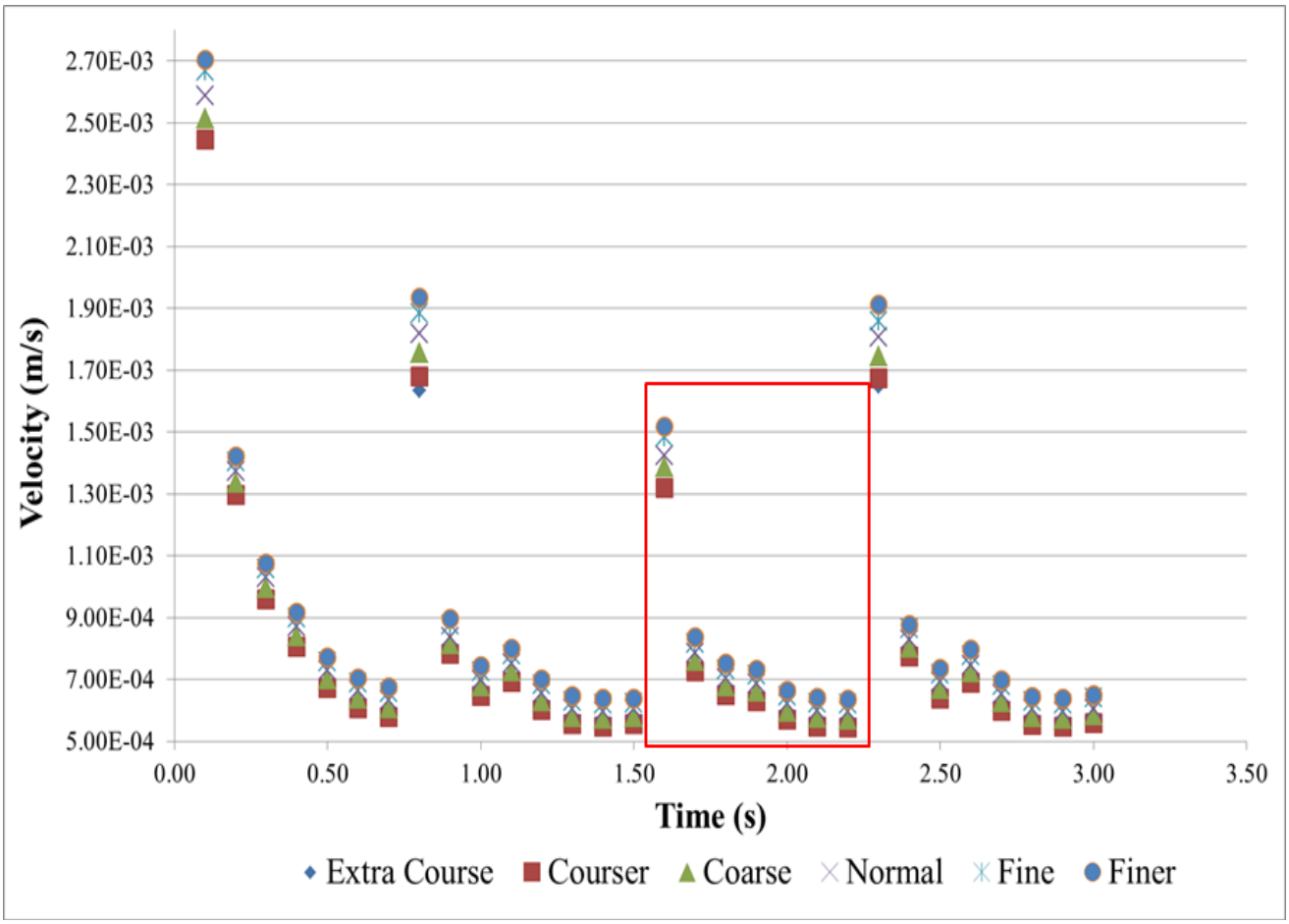

Figure B2: *<u>Mesh convergence comparing velocity and time:</u> The above plot shows the mesh convergence for the average velocity at the end of the large outlet vessel plotted against time. The plot shows that convergence occurs at the fine or normal mesh because the points are close to overlapping and the trend of velocity is consistently repeating. This also justifies using 2.25 seconds for modeling blood flow because after that point the oscillation amplitude is consistent. However, due to the length of computation, normal mesh was selected for further modeling.*

Appendix C: References

Blackshear, W M., Phillips, D J., Chikos, P M., Harley, J D., Thiele, B L., Strandness, D E. (1980). Carotid artery velocity patterns in normal and stenotic vessels. *Stroke, 11(1),* 67-71.

Carotid bifurcation. (2002, march 20). Retrieved from http://grabcad.com/library/carotid-bifurcation

Datta, A., & Rakesh, V. (2010). *An introduction to modeling of transport processes: application to biomedical systems*. New York: Cambridge University Press.

Elblbesy, M. A., Hereba, A. R. M., & Shawki, M. M. (2012). Effects of aspirin on rheological properties of erythrocytes in vitro. *International Journal of Biomedical Sciences, 8*(3).

Ino-Oka, E., Sekino, H., Kajikawa, S., Sato, T., & Inooka, H. (2009). Evaluation of carotid atherosclerosis from the perspective of blood flow reflection. *Clinical and Experimental Hypertension, 31*(3), 188-200. doi:10.1080/10641960902822443

Muraca, E., Gramigna, V., & Fragomeni, G. (2009). Mathematical Model of Blood Flow in Carotid Bifurcation. *Excerpt from the Proceedings of the COMSOL Conference 2009 Milan.*

Nguyen, K. T., Clark, C. D., Chancellor, T. J., & Papavassilioua, D. V. (2008). Carotid geometry effects on blood flow and on risk for vascular disease. *Journal of Biomechanics, 41*(1), 11-19. doi:10.1016/j.jbiomech.2007.08.012

Pruissen, M. O., Gerritsen, S. A., Prinsen, T. J., Dijk, J. M., Kappelle, L. J., & Algra, A. (2007). Carotid intima-media thickness is different in large- and small-vessel ischemic Stroke. *Stroke, 38,* 1371-1373.

Rajman, I., Eacho, P. I., Chowienczyk, P. J., & Ritter, J. M. (1999, August). LDL particle size: an important drug target? *Journal of Clinical Pharmacology, 48*(2), 125-143.

Sheth, V. & Ritter, A. (2010). Using computational fluid dynamics model to predict changes in velocity properties in stented carotid artery. *Excerpt from the Proceedings of the COMSOL Conference 2010 Paris.*

Rosenson, R. S. (2008). Treatment with aspirin and dipyridamole is more effective than aspirin in reducing low shear blood viscosity. *Microcirculation, 15*, 615-620. doi: 10.1080/10739680802229316

Studinger, P., Lenard, Z., Kovats, Z., Kocsis, L., & Kollai, M. (2003). Static and dynamic changes in carotid artery diameter in humans during and after strenuous exercise. *Journal of Physics, 550*(2), 575-583.

University of Maryland Medical Center. (2008). *Carotid artery surgery: Normal anatomy.* Retrieved April 18, 2013, from University of Maryland Medical System Web site: http://www.umm.edu/patiented/articles/carotid_artery_surgery_normal_anatomy_000124.htm

Vennemann, P., Lindken, R., & Westerweel, J. (2007). In vivo whole-field blood velocity measurement techniques. *Experiments in Fluids, 42*(4), 495-511. doi: 10.1007/s00348-007-0276-4

Wentzel, J. J., Chatzizisis, Y. S., Gijsen, F. J., Giannoglou, G. D., Feldman, C. L., & Stone, P. H. (2012). Endothelial shear stress in the evolution of coronary atherosclerotic plaque and vascular remodelling: current understanding and remaining questions. *Cardiovascular Research, 96*, 234-243.

Zarins, C K., Giddens, D P., Bharadvaj, B K., Sottiurai, V S., Mabon, R F. and Glagov, S. (1983). Carotid bifurcation atherosclerosis. Quantitative correlation of plaque localization with flow velocity profiles and wall shear stress. *Circulation Research, 53,* 502-514.